

An Estimator for Torque and Draft Force Requirements of a New Up-cut Rotary Tiller

I. Ahmadi^{1*}, M. Beigi²

Received: 18-03-2018

Accepted: 26-06-2018

Abstract

The aim of this study is to design, fabricate and evaluate a new type of up-cut rotary tiller and to develop correct formulas to estimate its torque and draft force using the laws of classical mechanics. In order to verify the model, a real-sized prototype of the rotary tiller was tested. It was hypothesized that four processes are involved to create the rotary tiller torque, namely soil cutting, soil lifting, soil-metal friction, and soil velocity. Furthermore, it was assumed that the horizontal components of soil cutting and soil-metal friction forces create the required draft of the machine. Based on these hypotheses, mathematical formulas were developed to calculate torque, and draft requirements of the machine. To facilitate performing necessary calculations, the developed formulas were entered in a worksheet of the MS Excel software. According to the results of this study, the average experimental draft and torque of the machine tilling a silty clay loam soil were 16.8 N and 12.8 Nm, respectively. Furthermore, the average theoretical draft and torque of the machine were 13 N and 11.8 Nm respectively. These promising results can be considered as the accuracy check of the formulas developed herein.

Keywords: Theoretical modeling, Torque and draft force measurement, Up-cut rotary tiller

Introduction

Imagine a gardener digging and turning over the orchard soil with a shovel. The shovel is a suitable tool in places where the lack of maneuverability is a serious issue. Is there an engine-powered machine that can perform the same? The rotary tiller can be an appropriate option. However, the working depth of a conventional down cut rotary tiller is restricted, and it may have undesirable side effects such as soil re-tilling. The up-cut rotary tiller is an alternative choice to compensate for the above-mentioned drawbacks of the conventional one (Shibusawa, 1993). In order to design a rotary tillage machine, it is important to have a correct understanding of the amount of torque required. To achieve this goal, the majority of researchers measured the

torque requirement or specific fuel consumption of a conventional rotary tiller using an experimental procedure (Asland Singh, 2009; Chertkiattipol and Niyamapa, 2010; Matin *et al.*, 2015, Gholami *et al.*, 2017), while few researchers calculated the machine torque theoretically (Bernacki *et al.*, 1972; Ahmadi, 2017). However, the experimental measurement as well as the theoretical calculation of the torque and draft requirements of an up-cut rotary tiller has not received the amount of attention that it deserves.

Therefore, the aim of this study is to design, fabricate and analyze experimentally a new up-cut rotary tiller and to estimate its torque and draft using the laws of classical mechanics.

Materials and Methods

Introducing the machine

The working unit of the machine consists of three main parts: blades, a flange, and a rotating shaft. Each blade is formed from a cutting edge and a blade extension. The blade extension is a curved metal shank with the inner radius of 140 mm, thickness of 20 mm,

1- Assistant Professor of Biosystems Engineering, Department of Plant Production and Genetics Engineering, Isfahan (Khorasgan) Branch, Islamic Azad University, Isfahan, Iran

2- Associate Professor of Biosystems Engineering, Department of Mechanical Engineering, Tiran Branch, Islamic Azad University, Tiran, Iran

(*- Corresponding Author Email: i_ahmadi_m@yahoo.com)

DOI: 10.22067/jam.v10i1.71744

width of 60 mm, and the central angle of 225° (Fig. 1a).

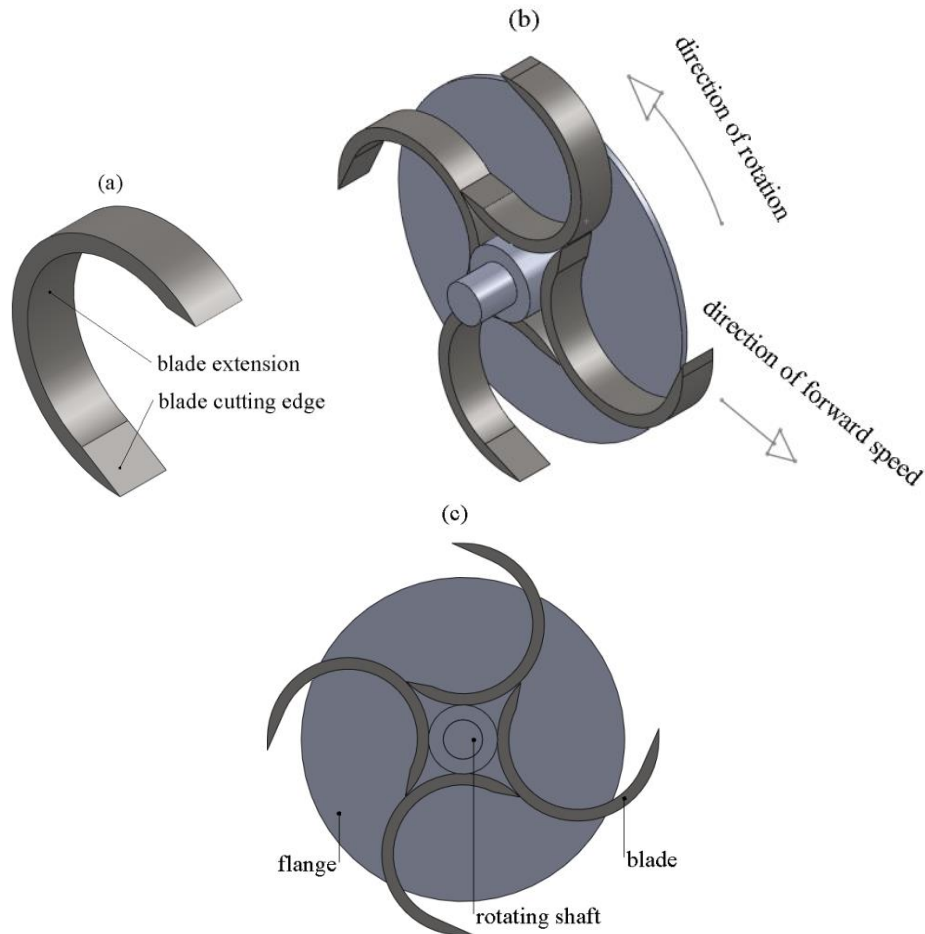


Fig. 1. a) Components of the designed blade, b) 3D, and c) 2D views of the working unit of the tiller

Figs. 1b and 1c depict the method of assembly of the blades on a flange. The end of each blade extension is located tangentially on the back of the blade ahead. During operation, it is expected that the cut soil flows through the blade extension passage as the flange rotates, then the soil is delivered to the back of the next blade extension, which finally discharges it behind the machine.

Introducing the test rig of the machine

After the fabrication of the machine prototype, it was installed on a test rig so that the translational motion of the tiller relative to the ground, as well as the effect of the operation of all blades on the draft force and torque requirements of the machine can be studied. The prototype had a simple manually operated soil bin. Maintaining a fixed speed ratio was the most important point considered for designing the test rig. Fig. 2 shows details of the test rig used herein.

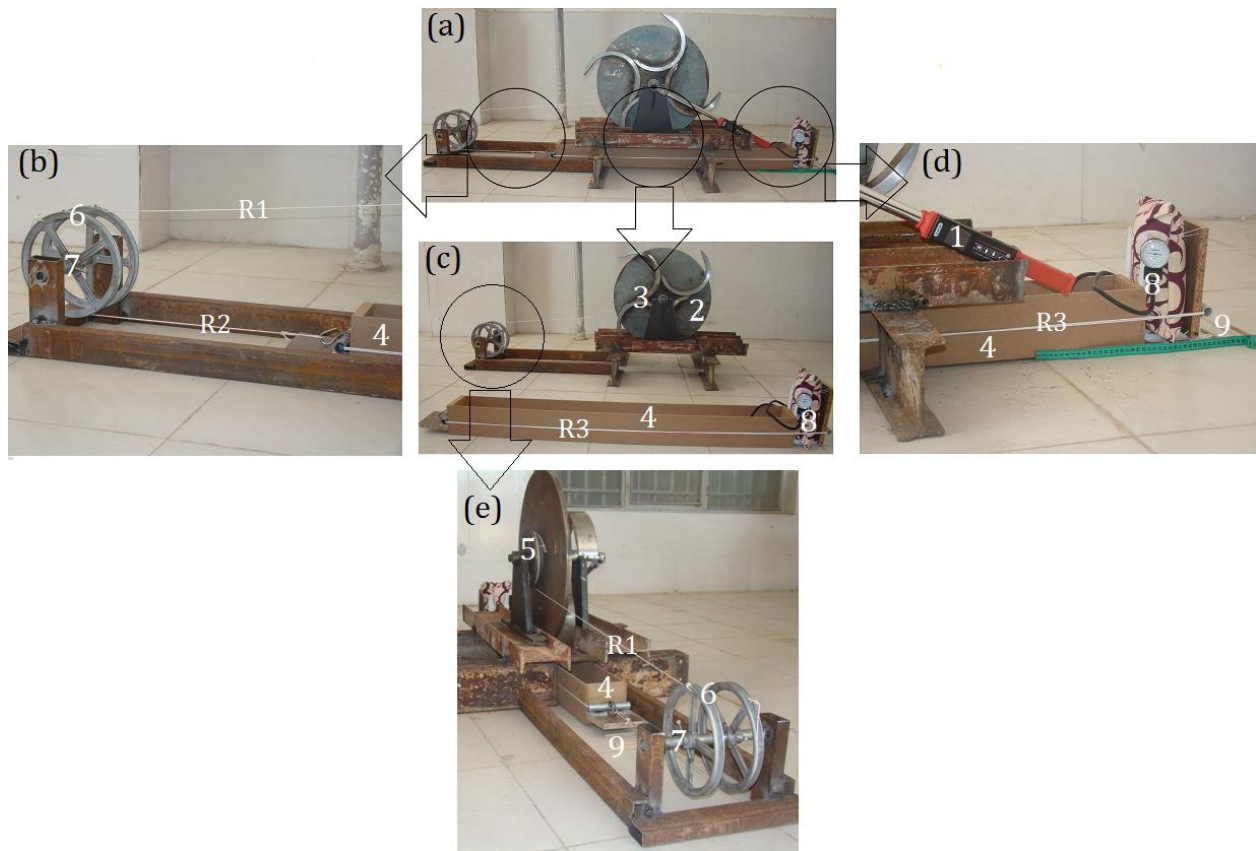


Fig.2. a) Complete assembly, b) magnified view of the front part, c) exploded view, d) magnified view of the rear part of the test rig, and e) the method of motion activation of the soil box. Where digit 1 was used for the digital torque wrench, 2 for the machine shaft and flange, 3 for each of the blades, 4 for the soil box, 5 for the shaft pulley, 6 for the twin pulleys, 7 for the shaft of the twin pulleys, 8 for the pressure sensor and gauge, and 9 for the soil box rollers. Furthermore, R1 was used for the rope that connects the shaft pulley to one of the twin pulleys, R2 for the rope that connects the other twin pulley to the rope R3 and R3 for the rope that surrounds both the pressure sensor and the soil box

The only power source of the test rig is the input torque, which is provided by a manually operated digital torque wrench 1. The resulting rotational motion is transferred through the shaft and flange 2 to the blades 3 of the machine, which were designed to cut the soil of the soil box 4. Pulley 5, which was fixed on the shaft, conveys power to one of the twin pulleys 6 through the rope R1. Because the twin pulleys were fixed to the free-rolling shaft 7, rotation of the first pulley leads to the rotation of the other, which in turn pulls the soil box 4 by means of the rope R2. To measure the required force for the motion of the soil box, a pressure sensor and gauge 8 was

utilized (Model: MDF[®] Calibra Aneroid Premium Professional Sphygmomanometer with the accuracy of ± 3 mmHg without pin stop), which were attached to the soil box using the rope R3. As shown, when the rope R2 pulls the surrounding rope R3, it makes the pressure sensor compressed against the backplane of the soil box 4; therefore, the pressure gauge 8 can measure the horizontal force developed in the soil cutting process. To reduce the friction between the soil box and the ground, free-rolling rollers 9 were used. In this assembly, the value of speed ratio, i.e. the ratio of the peripheral speed of the blade tip to the speed of the soil box, can be altered using

pulleys having different diameters. In the present arrangement of pulleys, the resulting speed ratio was 3.6. Finally, in order to extract the net torque required to cut the soil (T_c) from the total torque measured by the torque wrench 1 (T_t), the imposed torque to the wrench due to the motion of the soil box (T_m) was calculated: The required force for moving the soil box was named by F_m (N), then T_m (Nm) was calculated using the formula $T_m = F_m \times \frac{95}{1000}$, because all of the utilized pulleys had the radius of 95 mm. Finally, T_c can be calculated using the formula $T_c = T_t - T_m$.

An experiment was performed using a remolded silty clay loam soil (Table 1). The

average moisture content of the soil was about 10%. Before performing the test, the soil bed was prepared to achieve the desired level of cone penetration resistance i.e. maximum value of about 800 kPa with a cone penetrometer (Model CP20, Agridy Rimikpty. Ltd. Toowoomba, Australia) to a depth of 100 mm. Firstly, the soil was pulverized and water was sprayed on it to achieve the required moisture content. Then, the soil box was filled with the soil in three layers and each layer is leveled and compacted manually to the desired penetration resistance. To ensure uniformity of the soil, preparation of the soil bed was repeated if the penetration resistance values varied significantly from each other.

Table 1- General properties of the soil used for the verification procedure

Texture	Sand (%)	Silt (%)	Clay (%)	pH	EC	C (kPa)	ϕ (°)	δ (°)	ρ (kg m^{-3})	OMC (%)	Gs
Silty clay loam	18	42	40	6.5	1	10	25	12	1850	1.5	2.74

Estimation of the machine torque

It is hypothesized that, as followed below, four processes are involved to create the machine torque.

Torque requirement due to soil cutting process

To calculate the above-mentioned torque, the kinematics of the blade must be realized. To achieve this goal, the position coordinates

of the cutting edge of the working blade were obtained using eq. (1):

$$\begin{cases} x_{wb} = vt + R_b \sin \omega t \\ y_{wb} = -R_b \cos \omega t \end{cases} \quad (1)$$

Note: Definitions of the parameters used in the equations have been given in the Appendix 1.

The geometric path of the working blade (by setting $v = 1 \text{ m s}^{-1}$, $\omega = 10 \text{ rad s}^{-1}$ and $R_b = 0.33 \text{ m}$) has been shown in Fig.3a.

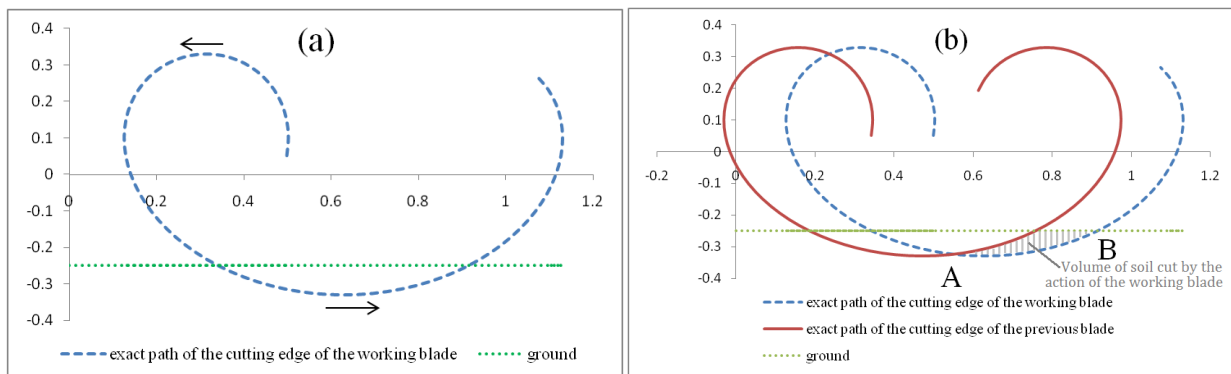


Fig.3. a) The path of the cutting edge of the working blade b) the relative positions of the working and previous blade paths

Since the geometric path of the cutting edge of the previous blade is known (eq.(2)), the volume of soil that is being cut by the working blade will be available.

$$\begin{cases} x_{pb} = vt + R_b \sin(\omega t + \frac{\pi}{2}) \\ y_{pb} = -R_b \cos(\omega t + \frac{\pi}{2}) \end{cases} \quad (2)$$

Simultaneous representation of the cutting edge paths of the working and the previous blades have been depicted in Fig.3b wherein it has been shown that the working blade cuts a narrow layer of soil in its operating cycle. Therefore, the weight (and ultimately the normal force) exerted on the soil failure plane is negligible. In other words, the required shearing force to cut the soil can be calculated using the formula $R_i = cA_i$. To calculate the torque requirement due to R_i using the MS Excel software, the curve AB (having a central angle of about 45°) has been divided into 5 segments (each having a central angle of 9°), and the length of each segment is denoted by

$S_i = \sqrt{(x_{wbi} - x_{wbi-1})^2 + (y_{wbi} - y_{wbi-1})^2}$, then the area of that segment of the failure plane as well as its corresponding soil shearing resistance can be calculated as $A_i = S_i \times d$ and $R_i = c \times A_i$. Multiplying R_i by $R_b \times \cos(\left| \tan^{-1}\left(\frac{R_b \omega \sin \omega t}{v + R_b \omega \cos \omega t}\right) - \omega t \right|)$ gives the

required instantaneous torque T_{ci} , and the torque requirement of a blade in one revolution of the rotor due to the soil cutting process (T_C) will be obtained using the

following formula: $\frac{\sum T_{ci} \times \frac{9\pi}{180}}{2\pi} = \frac{\sum T_{ci}}{40}$.

Torque requirement due to soil lifting and soil-metal friction processes

The shape of the blade extension is an arc of a circle. To calculate the torque requirement due to the soil lifting process, it was supposed that the circular arc of the blade extension is divided into 25 segments, each having a central angle of 9° . Moreover, the added soil to the blade extension is accumulated in the lowest segment as the flange rotates. As shown in Fig.4, the working radius of the tiller equals to the distance between the cutting edge of the blade and the center of the rotating shaft ($R_b = r + 2R$). From the viewpoint of soil motion along the blade extension, the circular arc of the blade extension can be divided into three regions (Fig. 4). The names of the regions are: soil accumulation region (five circular segments, each having a central angle of 9°), soil lifting region (fifteen circular segments, each having a central angle of 9°), and soil discharge region (five circular segments, each having a central angle of 9°).

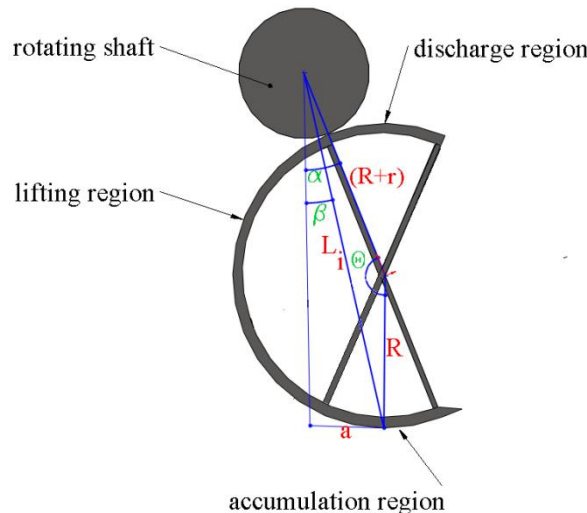


Fig.4. Three regions utilized for the calculation of torque requirement due to soil lifting process

If the position vector of the end of each circular segment (each of 25 circular arcs) is

known (\vec{L}_i), the instantaneous torque will be available using eq. (3):

$$\vec{T}_{wi} = \vec{L}_i \times \vec{W}_i = \vec{L}_i \times W_i \vec{j} = \vec{L}_i \times (-n W_u) \vec{j} \quad (3)$$

Where $W_u = \rho_{soil} g \frac{lb}{2} d R_b \frac{9\pi}{180}$. Parameter n is an integer with the values of 1, 3, 5, 7, and 9 for the accumulation region segments, 10, 9, 7, 5, 3, and 1 for the first six segments of the lifting region and 0 for the rest segments of it and the discharge region segments. Using the parameters shown in Fig.4, the calculating formula of \vec{L}_i is as follows (eq. (4)):

$$\left\{ \begin{array}{l} |L_i| = \sqrt{R^2 + (R+r)^2 - 2R(R+r)\cos\theta} \\ a = (R+r)\sin\alpha \\ \beta = \sin^{-1}\left(\frac{a}{L_i}\right) \\ \theta = 171^\circ \text{ to } -45^\circ (\text{step} - 9^\circ) \\ \alpha = 9^\circ \text{ to } 225^\circ (\text{step} + 9^\circ) \\ \vec{L}_i = |L_i|(\sin\beta\vec{i} + \cos\beta\vec{j}) = L_x\vec{i} + L_y\vec{j} \end{array} \right. \quad (4)$$

The same procedure can be used to calculate the torque requirement due to the soil-metal friction process. The only substitution in eq. (3) is the replacement of \vec{W}_i with \vec{F}_i , i.e.,

$$\vec{T}_{F_i} = \vec{L}_i \times \vec{F}_i = \vec{L}_i \times F_i\vec{i} = \vec{L}_i \times (-\mu n W_u)\vec{i} \quad (5)$$

Combining eqs. (3) and (5) gives:

$$\begin{aligned} \vec{T}_{WF_i} &= \vec{T}_{W_i} + \vec{T}_{F_i} = \vec{L}_i \times (\vec{W}_i + \vec{F}_i) \\ &= (L_x\vec{i} + L_y\vec{j}) \\ &\quad \times (W_y\vec{j} + F_x\vec{i}) \\ &= (L_x W_y - L_y F_x)\vec{k} \end{aligned} \quad (6)$$

Finally, the torque requirement due to combined soil lifting and soil-metal friction processes in one revolution of each blade can be obtained using eq. (7):

$$\vec{T}_{WF} = \frac{\sum(\vec{T}_{WF_i} \frac{9\pi}{180})}{2\pi} = \frac{\sum T_{WF_i}}{40} \quad (7)$$

Required dynamic torque

To calculate dynamic torque, the angular impulse and momentum method can be utilized. Eq. (8) demonstrates the formula. This formula is written for one of the above-mentioned 25 segments. Furthermore, suppose that the position vector (\vec{L}_i) and the soil mass (m_i) are constant values during the soil movement in each of 9° segments.

$$\begin{aligned} \vec{L}_i \times m_i \vec{V}_{i-1} + \vec{T}_{D_i} dt & \\ &= \vec{L}_i \times m_i \vec{V}_i \xrightarrow{\text{yields}} \vec{T}_{D_i} dt \\ &= \vec{L}_i \times m_i (\vec{V}_i - \vec{V}_{i-1}) \\ &\xrightarrow{\text{yields}} \vec{T}_{D_i} \\ &= \frac{m_i \vec{L}_i \times (\vec{V}_i - \vec{V}_{i-1})}{dt} \end{aligned} \quad (8)$$

In eq. (8), \vec{V}_i is the absolute value of soil velocity at the end of each circular segment, and dt is equal to $\frac{9\pi}{\omega}$. To calculate \vec{V}_i , the absolute position vector of soil at the end of each segment must be available (eq. (9)):

$$\begin{cases} \vec{X}_i = (vt + |L_i| \sin \omega t)\vec{i} \\ \vec{Y}_i = -|L_i| \cos \omega t \vec{j} \end{cases} \quad (9)$$

The first derivative of eq. (9) leads to the absolute velocity of soil at the end of each circular segment, i.e.:

$$\begin{cases} \vec{V}_{x_i} = (v + |L_i| \omega \cos \omega t)\vec{i} \\ \vec{V}_{y_i} = |L_i| \omega \sin \omega t \vec{j} \end{cases} \quad (10)$$

Applying the specifications of the vector product, the value of \vec{T}_{D_i} can be calculated using eq. (11):

$$\vec{T}_{D_i} = \frac{m_i(L_x\vec{i} + L_y\vec{j}) \times [(v_{x_i} - v_{x_{i-1}})\vec{i} + (v_{y_i} - v_{y_{i-1}})\vec{j}]}{dt} = \frac{m_i(L_x(v_{y_i} - v_{y_{i-1}}) - L_y(v_{x_i} - v_{x_{i-1}}))\vec{k}}{dt} \quad (11)$$

Finally, the required dynamic torque in one revolution of a blade can be calculated as follows:

$$\vec{T}_D = \frac{\sum \vec{T}_{D_i}}{40} \quad (12)$$

Now, since all of the torque requirements in one revolution of a blade are known (i.e., \vec{T}_C , \vec{T}_{WF} , and \vec{T}_D), the total torque of a blade (\vec{T}) can be calculated by summing them. Furthermore, the total torque of a flange (\vec{T}_F) and the total torque of the tiller (\vec{T}_T) can be obtained as follows:

$$\begin{cases} \vec{T}_F = N_b \vec{T} \\ \vec{T}_T = N_f \vec{T}_F \end{cases} \quad (13)$$

To facilitate performing calculations, the formulas developed herein were entered in a worksheet of the MS Excel software, where you can alter the values of five independent

parameters and observe the updated results and charts by pressing the Enter key (refer to the supplementary file).

Estimation of the machine draft theoretically

In order to estimate the draft force of the machine theoretically, horizontal components of soil cutting force and soil-metal friction force were calculated and summed. It should be noted that since the soil weight is directed down and the values of inertial force and moment of the cut soil are negligible in comparison with the corresponding items of the machine, the effect of soil weight and speed on the machine draft were neglected. The procedure for calculating the two components of the draft is summarized here:

- Dividing the time span from the instant when the rotating blade meets the soil to the instant when it reaches to the ground surface into five equally sized segments, and calculating the corresponding length of soil that is cut during each of them (S_i).

- Calculating the horizontal component of soil cutting force i.e. $F_{cxi} = c \times S_i \times d \times \cos\left(\left|\tan^{-1}\left(\frac{R_b \omega \sin \omega t}{v + R_b \omega \cos \omega t}\right) - \omega t\right|\right)$, and the horizontal component of soil-metal friction force i.e. $F_{fxi} = \mu n W_u$ for each time segment.

- Summing $F_{cxi}S$ and $F_{fxi}S$ to calculate SF_{cx} and SF_{fx} .

- Multiplying SF_{cx} and SF_{fx} by $\frac{9\pi}{180} = \frac{1}{40}$ to achieve average values of soil cutting force and soil-metal friction force.

Results and Discussion

Comparison of torque and draft curves of a single blade

Fig.5a shows the distribution of the theoretically obtained soil cutting-induced and the soil motion-induced torque curves of a blade over one revolution of the tiller shaft. The soil motion-induced torque consists of soil lifting, friction, and dynamic torques, and the sum of soil cutting and soil motion-induced torques composes the machine torque. The theoretical curves were obtained by entering the following values as the model input parameters: $c = 10 \text{ kPa}$, $v = 0.01 \text{ m s}^{-1}$, $\omega =$

0.1 rad s^{-1} , $R = 0.14 \text{ m}$, $r = 0.05 \text{ m}$, $d = 0.04 \text{ m}$, $\mu = 0.2$, and $\rho = 1850 \text{ kg m}^{-3}$. The theoretical soil-cutting-induced torque was about 9 Nm on part AB of the curve, which is exactly over the soil-cutting period. Then, it falls to zero and remains zero on part CD, where the working blade is not in contact with the soil. Finally, when the blade encounters the soil at the beginning of the next rotation of the blade, the curve jumps up to reach point E. On the other hand, the variation of the soil motion-induced torque starts from zero at F, where the working blade just touches the soil. Since there is no mass on the blade extension at F, all components of the soil motion-induced torque are zero at this point. The curve goes up from F to reach the largest value of about 6 Nm at G ($\alpha \cong 55^\circ$), and then it falls down and intersects the horizontal axis at H ($\alpha \cong 100^\circ$). The soil motion-induced torque remains zero between points H and I ($\alpha \cong 100^\circ - 360^\circ$) because the blade extension does not carry any soil in this range.

Figs. 5b and 5c depict the distribution of theoretical as well as experimental curves of the machine torque and the draft force of a blade over one revolution of the tiller shaft, respectively. The proximity of theoretical curves to the experimental ones can be considered as the verification of the developed formulas. As shown, both of the torque curves have zero values after rotation of the tiller shaft through the angle of 90° . This observation can be explained from this point that after rotation of the shaft through this rotation angle, almost all of the cut soil dropped from the blade surface; therefore, because the mass of soil supported by the blade was negligible, its corresponding soil motion-induced torque had zero values, too. In order to explain why the draft curves have zero values after the tiller shaft rotated about 50° , it is necessary to consider that the draft force is created from the interaction between the blade and the uncut soil. Because the blade is in contact with the uncut soil only in the first 50° of the shaft rotation, it is expected to have zero values for the draft force after this rotation angle.

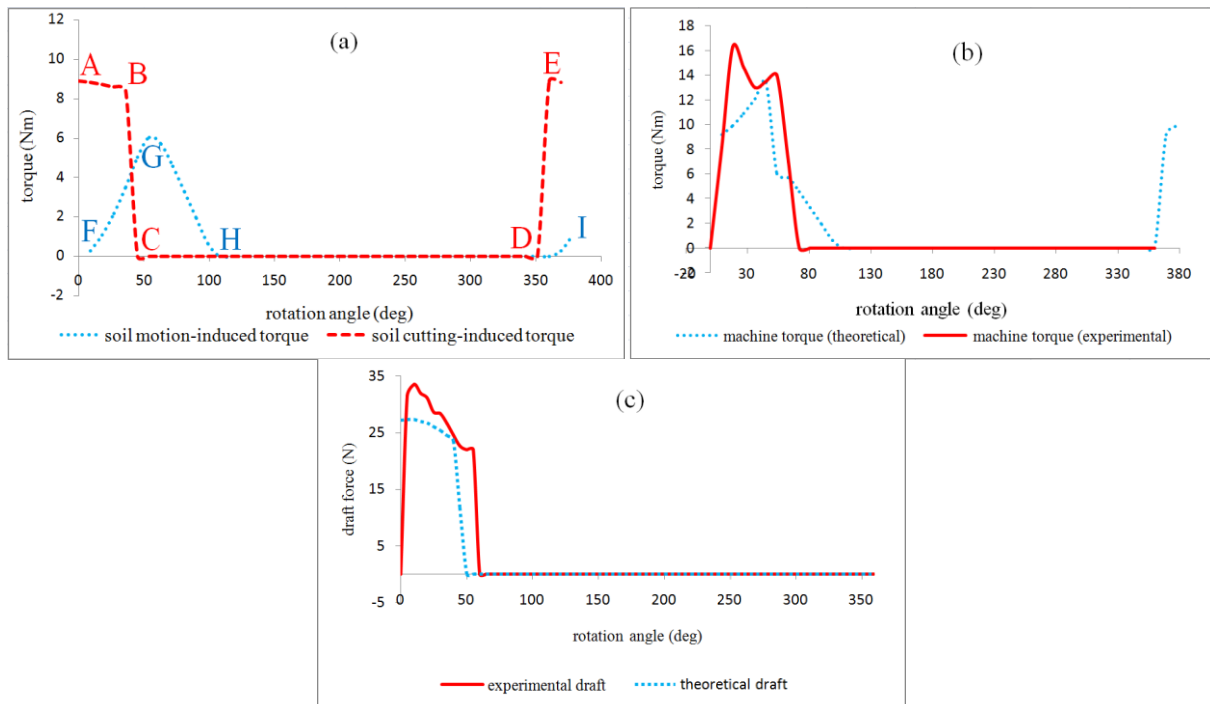


Fig.5. Comparison of a) theoretically estimated soil cutting and soil motion-induced torque curves b) theoretical and experimental curves of the machine torque, and c) theoretical and experimental draft curves of a blade

Furthermore, the average theoretical machine torque of a blade is around 2.95 Nm and the average experimental machine torque is about 3.2 Nm. Moreover the average theoretical draft force of a blade is around 3.25 N and the average experimental draft force is about 4.2 N. The difference between the average theoretical and experimental torques as well as draft forces may be due to dissimilarity in the working conditions of the modeled and real machines, the difference in the properties of the study soil, and the effect of unconsidered or neglected processes for the development of the theoretical formulas.

Effect of all blades on the torque requirements of the machine

Fig.6 shows the variation of the total, draft-induced and machine torques as a function of the angular position of the tiller shaft.

An important result obtained from Figure 6 regarding the design of the tiller is that in order to have a durable machine, the number of the tiller blades should be doubled because

there are angular spans in the charts where the torque requirement is zero. These angular spans, which are exactly matched with the time spans when no blade is in contact with the soil, make the curves to have a periodic up and down variation. This means that the torque requirement of the machine have a periodic nature, which leads to the vibration of the machine and ultimately makes the tiller to fail sooner. However, if the number of the tiller blades is doubled, the valleys of curves will be filled, which means that the machine will work with fewer vibrations. In order to double the number of blades without affecting the configuration of them, the new blade gang, having the same arrangement as the first, should be installed on the other side of the tiller flange. Moreover, each blade of the new gang should be welded to the flange exactly halfway of each circular arc between the two adjacent blades of the first gang.

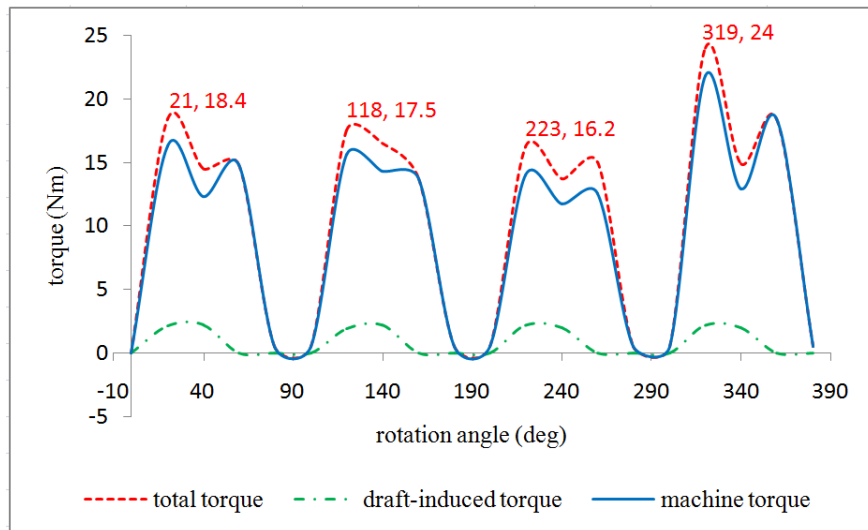


Fig. 6. Experimentally measured torque curves of the machine over one revolution of the tiller shaft

Conclusions

In this study, the soil engaging components of a new up-cut rotary tiller were designed and fabricated and the torque and draft force requirements of the machine were formulated using the laws of classical mechanics. The comparison of the calculated theoretical torque and draft force with the experimental ones had promising results that can be considered as the verification of the formulas developed herein (From a quantitative viewpoint, the average experimental draft and torque of the machine tilling a silty clay loam soil were 16.8 N and

12.8 Nm, respectively). Furthermore, the average theoretical draft and torque of the machine were 13 N and 11.8 Nm respectively. The outputs obtained from the formulas (driving torque of the machine and required draft force of it) can be used to design the transmission system of the machine.

Acknowledgment

The authors are grateful to the anonymous reviewers who devoted their valuable time to inspect this manuscript.

References

1. Ahmadi, I. 2017. A torque calculator for rotary tiller using the laws of classical mechanics. *Soil & Tillage Research* 165: 137-143.
2. Asl, J.H., and S. Singh. 2009. Optimization and evaluation of rotary tiller blades: computer solution of mathematical relations. *Soil & Tillage Research* 106: 1-7.
3. Bernacki, H., J. Haman, and Cz. Kanafojski. 1972. *Agricultural machines, theory and construction*. Scientific publications foreign co-operation center of the CISTEI. Warsaw.
4. Chertkiattipol, S., and T. Niyamapa. 2010. Variations of torque and specific tilling energy for different rotary blades. *International Agricultural Engineering Journal* 19 (3): 1-14.
5. Gholami, H., D. Kalantari, and M. Rajabi Vandechali. 2017. Testing and evaluation of a rototiller with new ridged blades. *Journal of Agricultural Machinery* 7 (1): 26-36. (In Farsi).
6. Matin, M.A., J. M. Fielke, and J. M. A. Desbiolles. 2015. Torque and energy characteristics for strip-tillage cultivation when cutting furrows using three designs of rotary blade. *Biosystems Engineering* 129: 329-340.
7. Shibusawa, S. 1993. Reverse rotational rotary tiller for reduced power requirement in deep tillage. *Journal of Terramechanics* 30 (3): 205-217.

Appendix 1-Definition of the parameters used in the theoretical formulas

Item	Definition (unit)
L_i	Distance between the end point of the i-th segment of the blade extension and the center of rotor (m)
N_b, N_f	Number of blades per flange and number of flanges (-)
R_i	Shearing resistance of soil located close to the i-th segment of the blade path through the soil (N)
S_i and A_i	Length (m) and area (m ²) of the i-th segment of the blade path
T_{ci}	Torque supplied for cutting the soil located close to the i-th segment of the blade path through the soil (Nm)
$T_{wi},$ $T_{Fi}, T_{WFi},$ and T_{Di}	Torques supplied respectively to the soil lifting, overcoming the soil-metal friction, combined soil lifting and overcoming the soil-metal friction, and dynamic motion of the soil located close to the i-th segment of the blade extension (Nm)
V_i	Absolute velocity of the soil located close to the i-th segment of the blade extension (m s ⁻¹)
W_i and F_i	The weight of, and the friction force exerted on the soil located close to the i-th segment of the blade extension (N)
W_u	The weight of soil that enters to the first segment of the blade extension (N)
X_i, Y_i	The X and the Y components of the absolute position of the soil located close to the i-th segment of the blade extension (m)
\vec{i}, \vec{j}	Unit vectors along the x and the y axes, respectively
m_i	The mass of the soil located close to the i-th segment of the blade extension (kg)
x_{wb}, y_{wb}	The x and the y position coordinates of the cutting edge of the working blade (mm)
x_{pb}, y_{pb}	The x and the y position coordinates of the cutting edge of the previous blade (mm)
c	Soil cohesion (kPa)
d	Blade width (m)
lb	Bite length of the blade (m)
$r, R,$ and R_b	The rotating shaft radius, the blade extension radius, and the distance between the cutting edge of the blade and the rotating shaft center, respectively (m)
t	Time (s)
v	Forward speed of the machine (m s ⁻¹)
μ	Coefficient of soil-metal friction (-)
ω	Angular velocity of the rotor (rad s ⁻¹)

تخمینگر گشتاور و مقاومت کششی روتیواتور چرخش معکوس جدید

ایمان احمدی^{۱*}، محسن بیگی^۲

تاریخ دریافت: ۱۳۹۶/۱۲/۲۷

تاریخ پذیرش: ۱۳۹۷/۰۴/۰۵

چکیده

هدف از پژوهش حاضر طراحی، ساخت و ارزیابی یک نمونه جدید از روتیواتور چرخش معکوس، همچنین توسعه فرمول‌های صحیح برای تخمین نیازهای گشتاوری و نیرویی آن با استفاده از قوانین مکانیک کلاسیک است. به منظور تایید مدل، نمونه اولیه دستگاه مورد آزمون قرار گرفت. فرض شد که چهار فرآیند در ایجاد گشتاور مورد نیاز ماشین دخالت دارند که عبارتند از: برش خاک، بالا برده شدن خاک، اصطکاک بین خاک و فلز و سرعت خاک. از سوی دیگر فرض گردید که مؤلفه افقی نیروی برش و اصطکاک بین خاک و فلز در ایجاد مقاومت کششی مورد نیاز ماشین نقش دارند. بر مبنای این فرض‌ها، فرمول‌های ریاضی برای تخمین نیازهای گشتاوری و مقاومت کششی ماشین توسعه داده شد. برای تسهیل در انجام محاسبات، فرمول‌ها وارد نرم‌افزار اکسل شد. بر مبنای نتایج این پژوهش مقاومت کششی و گشتاور متوسط اندازه‌گیری شده برای خاک‌ورزی خاک دارای بافت لوم رسی سیلت‌دار به ترتیب برابر با ۱۶/۸ نیوتن و ۱۲/۸ نیوتن‌متر به دست آمد. به علاوه مقاومت کششی و گشتاور متوسط تخمین زده شده به ترتیب برابر با ۱۳ نیوتن و ۱۱/۸ نیوتن‌متر به دست آمد. شباهت مقادیر تخمین زده شده به مقادیر اندازه‌گیری شده بیانگر صحت فرمول‌های توسعه یافته در این پژوهش می‌باشد.

واژه‌های کلیدی: اندازه‌گیری گشتاور و مقاومت کششی، گاواهن دوار چرخش معکوس، مدل‌سازی تئوری

۱- استادیار مکانیک بیوسیستم، گروه مهندسی تولید و ژنتیک گیاهی، دانشگاه آزاد اسلامی، واحد اصفهان (خوراسگان)، اصفهان، ایران

۲- دانشیار مکانیک بیوسیستم، گروه مهندسی مکانیک، دانشگاه آزاد اسلامی، واحد تیران، تیران، ایران

*- نویسنده مسئول: (Email: i_ahmadi_m@yahoo.com)

